A Comprehensive Model for Solid-State Polycondensation of Poly(ethylene terephthalate): Combining Kinetics with Crystallization and Diffusion of Acetaldehyde

XIA-QIN WANG, DE-CHUN DENG

Chemical Engineering, College of Environmental Science and Engineering, Donghua University, 1882 West Yan-an Road, Shanghai, 200051, China

Received 23 October 2000; accepted 14 May 2001

ABSTRACT: A comprehensive mathematical model was established by considering the main and side reactions for solid-state polycondensation of poly(ethylene terephthalate). The effect of temperature on chain mobility was used to estimate the rate constants of chemical reactions. The polymer crystalline fraction was modeled as containing only repeat units, thus concentrating end groups and condensates in the amorphous fraction. The diffusion coefficient of acetaldehyde was calculated by the model. The simulation results of this comprehensive model were validated by experimental data reported in literature. The model predictions were important clues for further experimental study on poly(ethylene terephthalate) solid-state polycondensation. © 2002 John Wiley & Sons, Inc. J Appl Polym Sci 83: 3133–3144, 2002; DOI 10.1002/app.10113

Key words: solid-state polymerization; PET; mathematical model

INTRODUCTION

Poly(ethylene terephthalate) (PET) is one of the most important engineering thermoplastics because of its ability to orient and mold in different forms. Engineering applications of PET are, however, limited by the molecular weight of commercial resins. The limit is dictated by the nature of the molten state synthesis. One option to increase the molecular weight to higher levers is the solid-state polycondensation (SSP) process, even though it takes a somewhat long reaction time.

SSP processes are carried out by heating PET precursors with lower molecular weight in a flow of inert gas or under vacuum at a temperature below the crystalline melting point but well above the glass transition temperature. The main chemical reactions that take place during SSP are esterification and *trans*-esterification (ester interchange) in which water and ethylene glycol are released as byproducts. To increase the rate of these reactions, the removal of byproducts by diffusion out of the solid semicrystalline polymer is necessary. So, the polycondensation rate in the solid state depends on both chemical and physical processes and is determined by the slower process.

PET SSP has witnessed both an extensive and an intensive progress with a wealth of experimental investigations[1–4] on SSP of PET reported in literature and some models[5–8] with limited utility proposed. Ravindranath and Mashelkar[9] comprehensively analyzed some previous models and, by assuming that all polymer chains had only ethylene glycol ends, developed a model considering both transesterification reaction and physical dif-

Correspondence to: X.-Q. Wang.

Contract grant sponsor: Fok Ying Tung Education Foundation.

Journal of Applied Polymer Science, Vol. 83, 3133–3144 (2002)

Table I Kinetics Scheme of Main and Side Reactions for PET SSP[11]

Reaction No.	Reactions	Forward, Reverse (Rate Constants)
1	EG + TPA ⇌ tEG + tTPA + W	k_1, k_1/K_1
2	EG + tTPA ⇌ tEG + bTPA + W	k_2, k_2/K_2
3	tEG + TPA ⇌ bEG + tTPA + W	k_3, k_3/K_3
4	tEG + tTPA ⇌ bEG + bTPA + W	k_4, k_4/K_4
5	tEG + tEG ⇌ bEG + EG	k_5, k_5/K_5
6	tEG + tEG → bEG + W	k_6
7	bEG + bTPA → tVIN + tTPA	k_7
8	tEG + bTPA → AA + tTPA	k_8
9	tEG + tVIN → bEG + AA	k_9

fusion of ethylene glycol during PET SSP process. Tang et al.[10] improved Ravindranath and Mashelkar's model by adding an esterification reaction; they thought that transesterification and esterification occurred simultaneously and assumed the diffusion process of ethylene glycol and water is of Fickian type.

Kang[11] provided additional insight into the mechanism of PET SSP. Nine reactions and ten components, the effect of temperature and chain entanglement on chain mobility, were considered in his model. Mallon and Ray[12] stated that PET SSP took place only in the amorphous portion of semicrystalline polymer and that the melt polymerization kinetics of PET were employed in the amorphous phase.

It is generally accepted that SSP occurs only in the amorphous phase of solid polymer. The mobility of chain segments and end groups is considerably restricted in comparison with the situation in the melt. The activation energies of a polycondensation reaction in the melt are lower than the ones in the solid state.[13] Therefore, it may be not accurate to deal with the PET SSP in amorphous phase as purely melt polycondensation in existing PET SSP models.

This study is a continuation of the earlier works pertaining to the modeling of PET SSP process. It is aimed at providing better understanding of the mechanism of SSP for improving the model predictability and establishing a new comprehensive model. In this model, it is assumed that the physical diffusion of condensates (e.g., ethylene glycol, water, and acetaldehyde) will lead to the mass loss of the SSP system and crystallization during SSP will affect the reaction rates and equilibrium. The experimental evidence of the influence of PET precursor catalysts on SSP is submitted and the optimization of PET SSP is also discussed for any possible decrease of the processing time to enhance the industrial significance of SSP.

Table II Molecular Structures of Each Component

Symbol	Description	Molecular Structure
TPA	Terephthalic acid	HOOC—C$_6$H$_4$—COOH
EG	Ethylene glycol	$HOCH_2CH_2OH$
W	Water	H_2O
tEG	EG end group	$HOCH_2CH_2O\sim$
tTPA	TPA end group	HOOC—C$_6$H$_4$—CO~
bEG	EG repeat unit	$\sim OCH_2CH_2O\sim$
bTPA	TPA repeat unit	~OC—C$_6$H$_4$—CO~
bDEG	Diethylene glycol repeat unit	$\sim OCH_2CH_2OCH_2CH_2O\sim$
tVIN	Vinyl end group	$CH_2{=}CHO\sim$
AA	Acetaldehyde	CH_3CHO

Table III Mass Balance Equations

$$\frac{\partial C_{\mathrm{TPA}}}{\partial t} = (1-x_c)G_{\mathrm{TPA}}(t) + \frac{\partial C_{\mathrm{TPA}}}{\partial M}\frac{dM}{dt} + \frac{\partial C_{\mathrm{TPA}}}{\partial x_c}\frac{dx_c}{dt}$$

$$\frac{\partial C_{\mathrm{TPA}}}{\partial M} = -\frac{C_{\mathrm{TPA}}}{1-x_c} \quad \frac{\partial C_{\mathrm{TPA}}}{\partial x_c} = -\frac{C_{\mathrm{TPA}}}{1-x_c}$$

$$\frac{\partial C_{\mathrm{EG}}}{\partial t} = D_{\mathrm{EG}}\left[\frac{\partial^2 C_{\mathrm{EG}}}{\partial r^2} + \frac{\lambda}{r}\frac{\partial C_{\mathrm{EG}}}{\partial r}\right] + (1-x_c)G_{\mathrm{EG}}(t) + \frac{\partial C_{\mathrm{EG}}}{\partial M}\frac{dM}{dt} + \frac{\partial C_{\mathrm{EG}}}{\partial x_c}\frac{dx_c}{dt}$$

$$\frac{\partial C_{\mathrm{EG}}}{\partial M} = -\frac{C_{\mathrm{EG}} - (1/0.062)}{1-x_c} \quad \frac{\partial C_{\mathrm{EG}}}{\partial x_c} = \frac{C_{\mathrm{EG}}}{1-x_c}$$

$$\frac{\partial C_W}{\partial t} = D_W\left[\frac{\partial^2 C_W}{\partial r^2} + \frac{\lambda}{r}\frac{\partial C_W}{\partial r}\right] + (1-x_c)G_W(t) + \frac{\partial C_W}{\partial M}\frac{dM}{dt} + \frac{\partial C_W}{\partial x_c}\frac{dx_c}{dt}$$

$$\frac{\partial C_W}{\partial M} = -\frac{C_W - (1/0.018)}{1-x_c} \quad \frac{\partial C_W}{\partial x_c} = \frac{C_w}{1-x_c}$$

$$\frac{\partial C_{t\mathrm{EG}}}{\partial t} = (1-x_c)G_{t\mathrm{EG}}(t) + \frac{\partial C_{t\mathrm{EG}}}{\partial M}\frac{dM}{dt} + \frac{\partial C_{t\mathrm{EG}}}{\partial x_c}\frac{dx_c}{dt}$$

$$\frac{\partial C_{t\mathrm{EG}}}{\partial M} = -\frac{\partial C_{t\mathrm{EG}}}{1-x_c} \quad \frac{\partial C_{t\mathrm{EG}}}{\partial x_c} = \frac{C_{t\mathrm{EG}}}{1-x_c}$$

$$\frac{\partial C_{t\mathrm{TPA}}}{\partial t} = (1-x_c)G_{t\mathrm{TPA}}(t) + \frac{\partial C_{t\mathrm{TPA}}}{\partial M}\frac{dM}{dt} + \frac{\partial C_{t\mathrm{TPA}}}{\partial x_c}\frac{dx_c}{dt}$$

$$\frac{\partial C_{t\mathrm{TPA}}}{\partial M} = -\frac{C_{t\mathrm{TPA}}}{1-x_c} \quad \frac{\partial C_{t\mathrm{TPA}}}{\partial x_c} = \frac{C_{t\mathrm{TPA}}}{1-x_c}$$

$$\frac{\partial C_{b\mathrm{EG}}}{\partial t} = G_{b\mathrm{EG}}(t) + \frac{\partial C_{b\mathrm{EG}}}{\partial M}\frac{dM}{dt} + \frac{\partial C_{b\mathrm{EG}}}{\partial x_c}\frac{dx_c}{dt}$$

$$\frac{\partial C_{b\mathrm{EG}}}{\partial M} = -\frac{C_{b\mathrm{EG}}}{1-x_c} \quad \frac{\partial C_{b\mathrm{EG}}}{\partial x_c} = \frac{C_{b\mathrm{EG}}}{1-x_c}$$

$$\frac{\partial C_{b\mathrm{TPA}}}{\partial t} = G_{b\mathrm{TPA}}(t) + \frac{\partial C_{b\mathrm{EG}}}{\partial M}\frac{dM}{dt} + \frac{\partial C_{b\mathrm{TPA}}}{\partial x_c}\frac{dx_c}{dt}$$

$$\frac{\partial C_{b\mathrm{TPA}}}{\partial M} = -\frac{C_{b\mathrm{TPA}}}{1-x_c} \quad \frac{\partial C_{b\mathrm{TPA}}}{\partial x_c} = \frac{C_{b\mathrm{TPA}} - (1/0.132)}{1-x_c}$$

$$\frac{\partial C_{b\mathrm{DEG}}}{\partial t} = G_{b\mathrm{DEG}}(t) + \frac{\partial C_{b\mathrm{DEG}}}{\partial M}\frac{dM}{dt} + \frac{\partial C_{b\mathrm{DEG}}}{\partial x_c}\frac{dx_c}{dt}$$

$$\frac{\partial C_{b\mathrm{DEG}}}{\partial M} = -\frac{C_{b\mathrm{DEG}}}{1-x_c} \quad \frac{\partial C_{b\mathrm{DEG}}}{\partial x_c} = \frac{C_{b\mathrm{DEG}} - (1/0.104)}{1-x_c}$$

$$\frac{\partial C_{t\mathrm{VIN}}}{\partial t} = (1-x_c)G_{t\mathrm{VIN}}(t) + \frac{\partial C_{t\mathrm{VIN}}}{\partial M}\frac{dM}{dt} + \frac{\partial C_{t\mathrm{VIN}}}{\partial x_c}\frac{dx_c}{dt}$$

$$\frac{\partial C_{t\mathrm{VIN}}}{\partial M} = -\frac{C_{t\mathrm{VIN}}}{1-x_c} \quad \frac{\partial C_{t\mathrm{VIN}}}{\partial x_c} = \frac{C_{t\mathrm{VIN}}}{1-x_c}$$

$$\frac{\partial C_{\mathrm{AA}}}{\partial t} = D_{\mathrm{AA}}\left[\frac{\partial^2 C_{\mathrm{AA}}}{\partial r^2} + \frac{\lambda}{r}\frac{\partial C_{\mathrm{AA}}}{\partial r}\right] + (1-x_c)G_{\mathrm{AA}}(t) + \frac{\partial C_{\mathrm{AA}}}{\partial M}\frac{dM}{dt} + \frac{\partial C_{\mathrm{AA}}}{\partial x_c}\frac{dx_c}{dt}$$

$$\frac{\partial C_{\mathrm{AA}}}{\partial M} = -\frac{C_{\mathrm{AA}} - (1/0.044)}{1-x_c} \quad \frac{\partial C_{\mathrm{AA}}}{\partial x_c} = \frac{C_{\mathrm{AA}}}{1-x_c}$$

$$\frac{dx_c}{dt} = k_c(x_{\max} - x_c)$$

$$\frac{dM}{dt} = 0.062D_{\mathrm{EG}}\left[\frac{\partial^2 C_{\mathrm{EG}}}{\partial r^2} + \frac{\lambda}{r}\frac{\partial C_{\mathrm{EG}}}{\partial r}\right] + 0.018D_{\mathrm{W}}\left[\frac{\partial^2 C_{\mathrm{W}}}{\partial r^2} + \frac{\lambda}{r}\frac{\partial C_{\mathrm{W}}}{\partial r}\right] + 0.044D_{\mathrm{AA}}\left[\frac{\partial^2 C_{\mathrm{AA}}}{\partial r^2} + \frac{\lambda}{r}\frac{\partial C_{\mathrm{AA}}}{\partial r}\right]$$

Table IV $G_j(t)$ of Component j

$G_{\mathrm{TPA}}(t) = -R_1 - R_2 + R_5$
$G_{\mathrm{EG}}(t) = -R_1 - R_3$
$G_{\mathrm{W}}(t) = R_1 + R_2 + R_3 + R_4 + R_6$
$G_{t\mathrm{EG}}(t) = R_1 + R_2 - R_3 - R_4 - 2R_5 - R_8 - R_9$
$G_{t\mathrm{TPA}}(t) = R_1 - R_2 + R_3 - R_4 + R_7 + R_8$
$G_{b\mathrm{EG}}(t) = R_3 + R_4 + R_5 - R_7 + R_9$
$G_{b\mathrm{TPA}}(t) = R_2 + R_4 - R_7 - R_8$
$G_{b\mathrm{DEG}}(t) = R_6$
$G_{t\mathrm{VIN}}(t) = R_7 - R_9$
$G_{\mathrm{AA}}(t) = R_8 + R_9$

Kinetic Scheme for PET SSP

In principle, all reactions involved in the melt polycondensation are also possible in SSP. According to the early work of Ravindranath et al.[14] and recent work of Kang[11], the kinetic scheme of nine main and side reactions is shown in Table I. The SSP process of PET, which presents an interesting diffusion–reaction–crystallization interconnection, will be analyzed in terms of the reactions between the reactive end groups and polymer chain segments. The end groups and chain segments appearing in the main and side reactions are listed in Table II. In Table I, k_i (i = 1–9) are forward rate constants and K_i (i = 1–5) are the equilibrium constants. Reactions 1–4 are the esterification reactions, and reaction 5 is the transesterification reaction. Reaction 6 is a side reaction of diethylene glycol (DEG) formation. Reactions 7 and 8 are the thermal degradation reaction and the acetaldehyde formation reaction, respectively. Reaction 9 is the vinyl end-group consumption reaction.

MASS BALANCE EQUATIONS

The regular folding of polymer chains forms the ordered crystal phase, whereas the end groups, condensates, catalyst, and the segment between the lamellae form the amorphous phase. The reactive end groups and chain segments in the amorphous phase will react if they collide, enabling both molecular weight and crystallinity to increase. The mass of the reaction system will decrease with the diffusion of three kinds of condensates, which has an influence on the reaction rate. The mass balance equations, which reflect the interconnection of diffusion–reaction–crystallization, are summarized in Table III.

Let j = TPA, EG, W, tEG, tTPA, bEG, bTPA, bDEG, tVIN, and AA; in Table III, C_j is the local concentration in amorphous phase of component j; t is the reaction time; D_j is the diffusion coefficient of component j; r is the distance from the center of a pellet; λ is the shape factor of pellets; $G_j(t)$ is the generation rate of C_j due to SSP and it can be expressed by the combination of nine main and side reactions R_i (i = 1–9). $G_j(t)$ and R_i are listed in Tables IV and V, respectively.

BOUNDARY AND INITIAL CONDITIONS

The relevant boundary and initial conditions for the mass balance equations are summarized as follows:

$$C_{\mathrm{EG}} = C_{\mathrm{EG}s}, \quad C_W = C_{Ws}, \quad C_{\mathrm{AA}} = C_{\mathrm{AA}s} \qquad \text{for } t > 0,\ r = r0 \quad (1)$$

$$\frac{dC_{t\mathrm{EG}}}{dt} = 0, \quad \frac{dC_{t\mathrm{TPA}}}{dt} = 0 \quad \text{for } t > 0,\ r = 0 \quad (2)$$

$$C_{\mathrm{TPA}} = C_{\mathrm{TPA0}}, \quad C_{\mathrm{EG}} = C_{\mathrm{EG0}}, \quad C_W = C_{W0},$$
$$C_{t\mathrm{EG}} = C_{t\mathrm{EG0}}, \quad C_{t\mathrm{TPA}} = C_{t\mathrm{TPA0}}, \quad C_{b\mathrm{EG}} = C_{b\mathrm{EG0}},$$
$$C_{b\mathrm{TPA}} = C_{b\mathrm{TPA0}}, \quad C_{b\mathrm{DEG}} = C_{b\mathrm{DEG0}}, \quad C_{t\mathrm{VIN}} = C_{t\mathrm{VIN0}},$$
$$C_{\mathrm{AA}} = C_{\mathrm{AA0}}, \quad x_c = x_{c0} \quad \text{for } t = 0,\ 0 < r < r0 \quad (3)$$

Table V Reaction Rate R_i

$$R_1 = \frac{4k_1}{(1-x_c)^2} C_{\mathrm{EG}} C_{\mathrm{TPA}} - \frac{k_1/K_1}{(1-x_c)^2} C_{\mathrm{W}} C_{\mathrm{TPA}} \frac{C_{t\mathrm{EG}}}{C_{t\mathrm{EG}} + C_{b\mathrm{EG}}}$$

$$R_2 = \frac{2k_2}{(1-x_c)^2} C_{\mathrm{EG}} C_{t\mathrm{TPA}} - \frac{2k_2/K_2}{(1-x_c)^2} C_{\mathrm{W}} C_{b\mathrm{TPA}} \frac{C_{t\mathrm{EG}}}{C_{t\mathrm{EG}} + C_{b\mathrm{EG}}}$$

$$R_3 = \frac{2k_3}{(1-x_c)^2} C_{t\mathrm{EG}} C_{t\mathrm{TPA}} - \frac{k_3/K_3}{(1-x_c)^2} C_{\mathrm{W}} C_{t\mathrm{TPA}} \frac{C_{b\mathrm{EG}}}{C_{t\mathrm{EG}} + C_{b\mathrm{EG}}}$$

$$R_4 = \frac{k_4}{(1-x_c)^2} C_{t\mathrm{EG}} C_{t\mathrm{TPA}} - \frac{2k_4/K_4}{(1-x_c)} C_{\mathrm{W}} C_{b\mathrm{TPA}} \frac{C_{b\mathrm{EG}}}{C_{t\mathrm{EG}} + C_{b\mathrm{EG}}}$$

$$R_5 = \frac{k_5}{(1-x_c)^2} C_{t\mathrm{EG}} C_{t\mathrm{EG}} - \frac{4k_5/K_5}{(1-x_c)} C_{\mathrm{EG}} C_{b\mathrm{EG}}$$

$$R_6 = \frac{k_6}{(1-x_c)^2} C_{t\mathrm{EG}} C_{t\mathrm{EG}}$$

$$R_7 = k_7 C_{b\mathrm{EG}} \frac{C_{b\mathrm{TPA}}}{C_{t\mathrm{EG}} + C_{b\mathrm{EG}}}$$

$$R_8 = \frac{k_8}{1-x_c} C_{t\mathrm{EG}} \frac{C_{b\mathrm{TPA}}}{C_{t\mathrm{EG}} + C_{b\mathrm{EG}}}$$

$$R_9 = \frac{k_9}{(1-x_c)^2} C_{t\mathrm{EG}} C_{t\mathrm{VIN}}$$

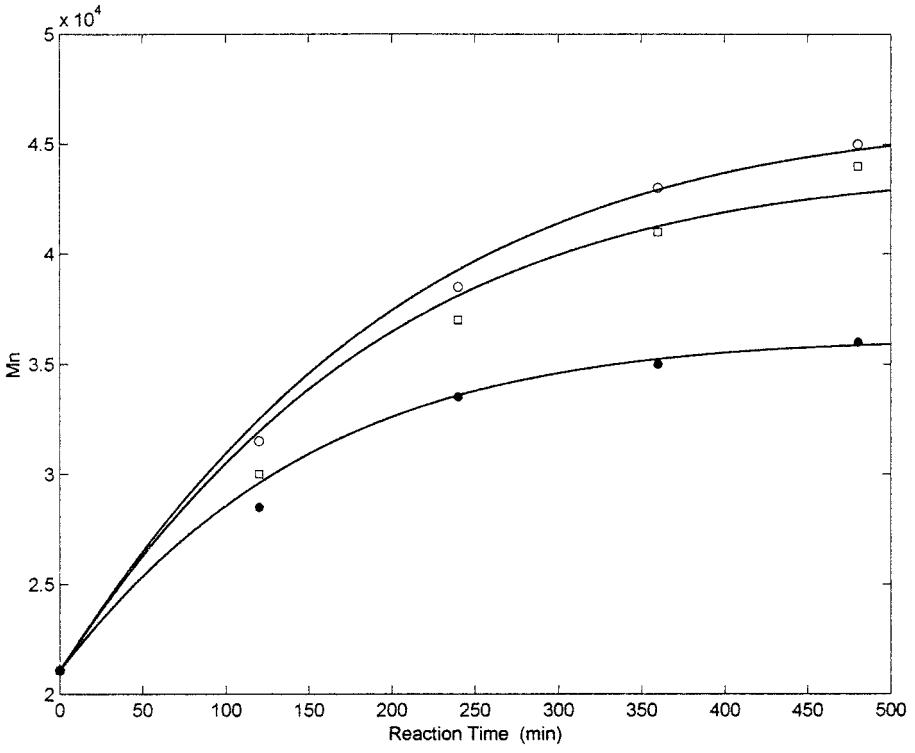

Figure 1. Estimation of the model parameters by fitting the model results against the experimental data of Jabarin and Lofgren[3]: (○) 230°C, (□) 220°C, (●) 210°C. The solid lines are calculated by the model by using the numerical parameters shown in Table VI.

where the subscripts 0 and s indicate the initial and interfacial value of the species; the concentration of volatile condensates at the surface was assumed to be zero. x_{c0} is the crystallinity of PET precursors and is assumed to be 0.3.

ASSUMPTIONS AND KINETIC PARAMETERS

Following the works of Ravindranath et al.[9], Kang,[11] Mallon and Ray,[12] and Li et al.,[15] a new model for the polycondensation of PET in the solid state is proposed in this work. The following assumptions are made.

1. Upon crystallization, polymer end groups, monomers, condensates, and catalysts are excluded from ordered crystalline region and exist exclusively in the amorphous phase. So, the reactions between end groups occur only in the amorphous portion of semicrystalline polymer and the molar concentration of noncrystallizing components will then increase because

Table VI Kinetic Parameters in the Mass Balance Equations[11,12,17]

$A_1 = A_2 = 2A_3$	$E_1 = E_2 = E_3$	$K_1 = K_2 = 2.5$
$A_3 = A_4 = 6.8 \times 10^{12}$ (L/mol)/min	$E_3 = E_4 = 17.6$ kcal/mol	$K_3 = K_4 = 1.25$
$A_5 = 5.4 \times 10^{12}$ (L/mol)/min	$E_5 = 18.5$ kcal/mol	$K_5 = 0.5$
$A_6 = 1.8 \times 10^{15}$ (L/mol)/min	$E_6 = 29.8$ kcal/mol	
$A_7 = 3.6 \times 10^{9}$ (L/mol)/min	$E_7 = 37.8$ kcal/mol	
$A_8 = 2.3 \times 10^{9}$ (L/mol)/min	$E_8 = E_6$	$E_p = 13.5$ kcal/mol
$A_9 = A_5$	$E_9 = E_6$	$D_{0AA} = 10.2 \times 10^{-5}$ cm^2/min[a]
$D_{0EG} = 18.6 \times 10^{-5}$ cm^2/min	$D_{0W} = 34.2 \times 10^{-5}$ cm^2/min	$k_c = 2.19 \times 10^{12}$exp(23186/RT)
$A = 0.39$	$B = 0.0025$ K^{-1}	

[a] D_{0AA} is calculated by our mathematical model.

Table VII The Major Characteristics of PET Precursors

Sample No.	1	2	3	4
Catalyst	$Sb_2(EG)_2$	$Sb_2(EG)_2$	Sb_2O_3	C-94
Inherent viscosity (dl/g)	0.641	0.649	0.636	0.643

Catalyst C-94 is based on hydrolytically stable titanium/silicon mixed oxides.

their accessible volume is now in the amorphous phase:

$$C_{\text{amorphous}} = C_{\text{overall}}/(1 - x_c) \quad (4)$$

This leads to higher observed reaction rates, and the equilibrium also shifts to higher conversions and chain length. The contribution of the amorphous phase in semicrystalline SSP was illustrated by the experimental observations of Simonova et al.[16]

2. Although the mobility of chain segments and end groups is considerably restricted in comparison with the situation in the melt, polymer chains have translational degrees of freedom, which are necessary for reactive end groups to diffuse in the amorphous phase to approach and react. Completion of the process in the solid state requires more time than in the melt. The chain mobility can be assumed to be of Arrhenius-type relationship:

$$m_p \propto \exp(-E_p/RT) \quad (5)$$

where m_p is the chain mobility at a temperature, and E_p is the activation energy of translational motion. This is very similar to the situation during crystallization where the chains have to translate to form the regular folding, which means the same activation energy of translational motion of polymer chains:

$$E_p = C_1 T/(C_2 + T - T_g) \quad (6)$$

Hence, considering the reaction rate to be proportional to the chain mobility, the rate constant k_i between two reactive polymer chains can be mathematically expressed as follows:

$$k_i = A_i \exp\left[\frac{-(E_p + E_i)}{RT}\right] \quad (i = 1\text{–}6 \text{ and } 9) \quad (7)$$

where A_i is the prefactor, and E_i is the activation energy for reaction i.

For intramolecular reactions 7 and 8, they are not affected by the translational motion of polymer chains, so the reaction rate constants can be expressed as:

$$k_i = A_i \exp\left[\frac{-E_i}{RT}\right] \quad (i = 7 \text{ and } 8) \quad (8)$$

The observed condensate diffusion coefficient is proportional to the amorphous fraction,

$$D_j = D_{0j}(1 - x_c) \quad (9)$$

Crystallization reduces the diffusion which, in turn, reduces the mass transport rate of byproducts. As for the secondary crystallization rate, we assume it is proportional to the crystallizable amorphous fraction:

$$\frac{dx_c}{dt} = k_c(x_{\max} - x_c) \quad (10)$$

$$x_{\max} = A + B(T - T_c) \quad (11)$$

Here, it is assumed that the molecular weight of PET has little effect on the rate of crystallization.

The target practice method is used to figured out D_{0AA}. A set of experimental measurements was selected[3], in which the initial concentration of AA, C_{AA0} is 24 ppm, and the concentration of residual AA after 6 hours' reaction at 200°C, C_{AAs} is 4.1 ppm. An arbitrary value of the diffusion

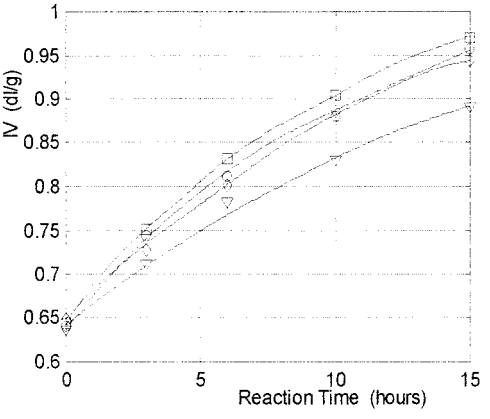

Figure 2. The influence of different precursor catalysts on inherent viscosity of polymer: (□) Sb (EG), (○) Sb (EG), (◇) SbO, (▽) C-94.

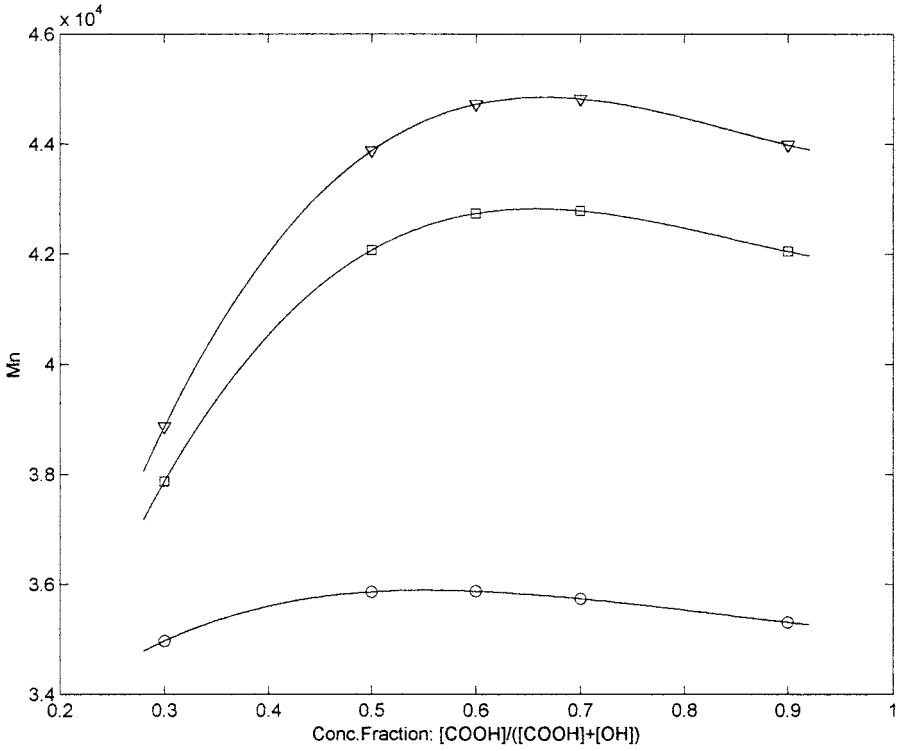

Figure 3. Number average molecular weight versus concentration fraction [COOH]/([COOH] + [OH]) at different temperatures: (▽) 230°C, (□) 220°C, (○) 210°C.

coefficient of AA, D_{0AA} was supposed and the calculation was made under the same conditions as those of the experimental measurements, C_{AA0} is 24 ppm. If the calculation results of C_{AAs} was not 4.1 ppm, another value of D_{0AA} was applied to the calculation. The process was repeated until C_{AAs} was 4.1 ppm and D_{0AA} of this time might be trustworthy. The best value of D_{0AA} was determined after the validity of D_{0AA} was checked with two other sets of experimental measurements.[3]

The numerical technique for solving the mass balance equations was the combination of the fourth Runge–Kutta method, which dealt with the time-interval integration and the finite difference method, which handled the integral divisions of the pellet.

RESULTS AND DISCUSSION

Confirmation of Mathematical Model

The model results are fitted against three experimental data sets of Jabarin and Lofgren[3] in Figure 1. All the parameters adjusted here are listed in Table VI. From Figure 1, it can be seen that the predicted values of number average molecular weight M_n agree well with the experimental measurement, although the catalyst effect of PET precursors on the reaction rates was not taken into account. Figure 1 also shows the temperature dependence of PET SSP. The reaction rates are controlled by chemical reactions and diffusion of condensates through the amorphous and crystal portion, both of which will be accelerated when the reaction temperature increases. The forward reaction rates surpass the backward reaction rate and high molecular weight is achieved. At lower temperature, the increase of molecular weight is not found to appreciate because of lower reaction rates of end groups and lower diffusion rates of condensates. Temperatures of industrial significance are some 5–50°C below the PET melting point.

Catalyst Effect of PET Precursors on SSP

It may be inconceivable that the catalyst effect of precursors on SSP is neglected in the mathematical model. Some experimental evidence is essential to test the predictability of the mathematical

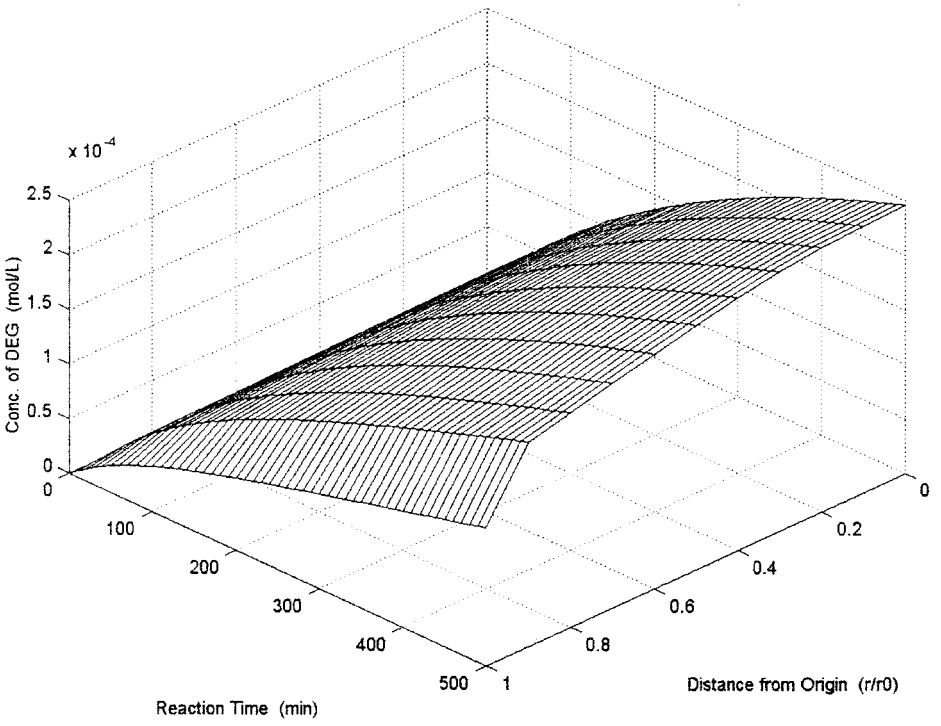

Figure 4. Distribution of concentration variance of DEG at different layers of a PET pellet under reaction temperature of 230°C.

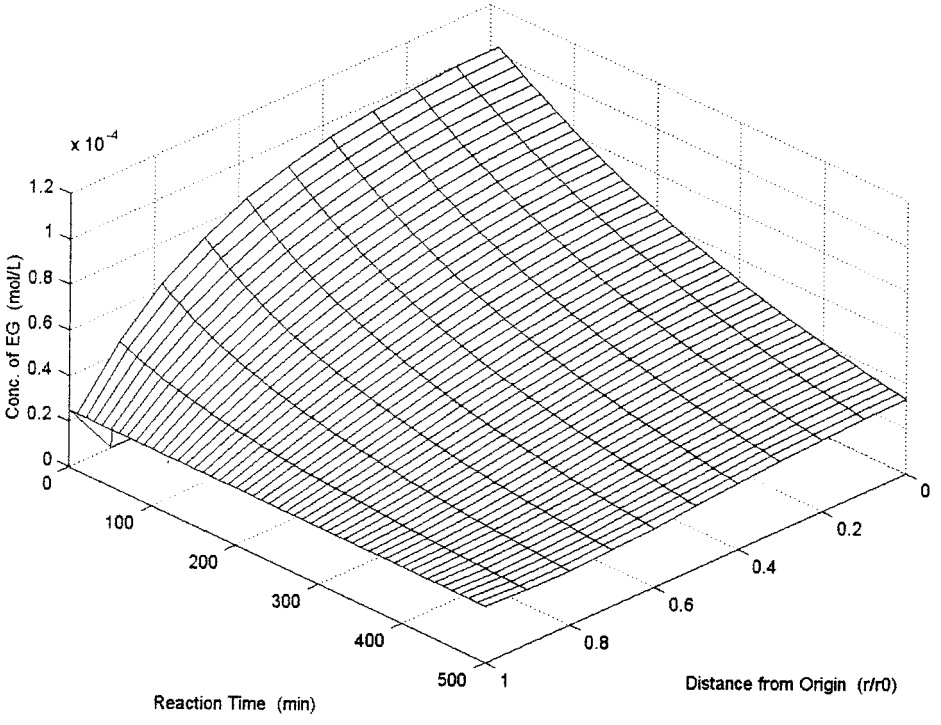

Figure 5. Distribution of concentration variance of EG at different layers of a PET pellet under reaction temperature of 230°C ($C_{EGs} = 0.25 \times 10^{-4}$ mol/L).

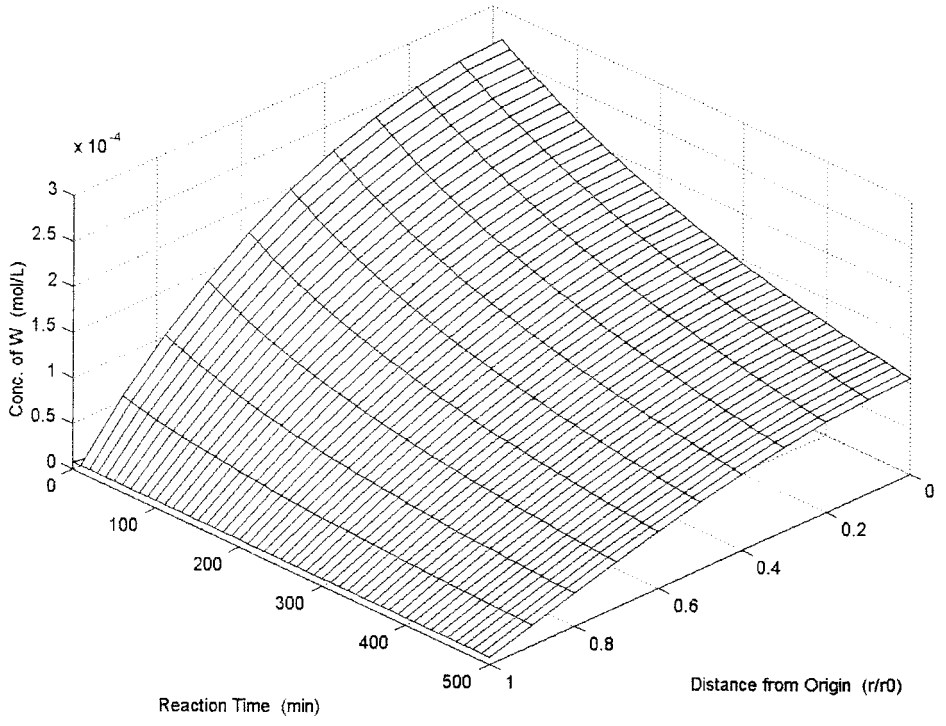

Figure 6. Distribution of concentration variance of water at different layers of a PET pellet under reaction temperature of 230°C ($C_{Ws} = 0.08 \times 10^{-4}$ mol/L).

model. Four kinds of PET precursor samples prepared with the same amount of catalysts are kindly provided by local polyester manufacturers, and the major characteristics of PET precursors are shown in Table VII.

Figure 2 reflects the influence of precursor catalyst on SSP. The experimental apparatus is a glass tube reactor embedded in a temperature-controllable electric heater. After 3 g PET pellet (the size of PET particles was about 0.3 cm^3) were placed into the reactor, the reactor was purged with N_2 (purity $>$ 99.99%) to obtain an oxygen-free environment. With continued nitrogen purge, the heater was then turned on and the temperature set point was set at 180°C for 20 min to precrystallize, which would avoid sticking at reaction temperature. Then, the temperature was raised and fixed at 210°C. The deviation of inherent viscosity (IV) is $<$9% when the reaction time is 10 h, and at the end of 15 h, the deviation is still $<$9%. The cause of the phenomenon is that the greatly restricted mobility of these catalysts makes them less active in solid state than corresponding molten state. The negligence of catalyst influence on SSP in existing mathematical models has not caused serious errors.

Influence of Concentration Ratio of End Groups

An ideal mathematical model not only reflects the whole process of PET SSP, but also suggests some information that at least gives new directions for further research. The main and side reactions occur simultaneously during SSP and the end groups affect PET SSP. The relation between number average molecular weight and the concentration ratio of end groups [tTPA/(tEG + tTPA), or [COOH]/([OH] + [COOH])] is depicted in Figure 3. All parameters adjusted here are listed in Table VI. The calculation results demonstrate that the molecular weight obtained through SSP achieves the highest value when the concentration ratio of end groups is about 0.6–0.7, or [COOH]/[OH] is about 2. The optimum value of concentration ratio of end groups coincides with the results of Zimmermann and coworkers,[18] who only considered transesterification reaction, disregarding diffusion and crystallization. The relation between polymer molecular weight and the concentration ration of end groups is perhaps a clue to enhance the industrial significance in producing polymer with very high molecular weight.

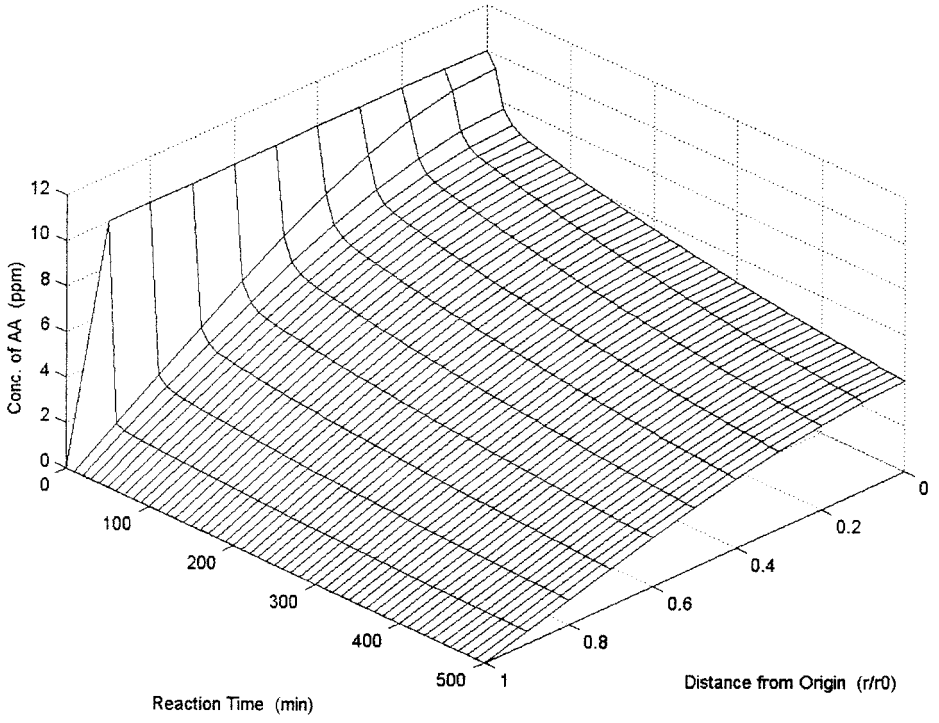

Figure 7. Distribution of concentration variance of acetaldehyde at different layers of a PET pellet under reaction temperature of 230°C (C_{AA0} = 10 ppm, C_{AAs} = 0 ppm).

Formation of DEG

The factors that affect PET sticking together mainly include DEG content in pellets, crystallization, and the concentration of oligomers. These factors have negative effects on many properties of practical interest, such as thermal and light stability, and hydrolytic, thermal, and oxidative degradation. The melting point of PET is greatly affected by DEG content. Reaction 6 in Table I is the DEG formation reaction, and Figure 4 describes the process of DEG formation during SSP when the reaction temperature is 230°C. The concentration of DEG becomes larger with the prolongation of SSP reaction time. Therefore, short reaction time is favorable for the quality of final product.

Distribution of Volatile Byproducts EG, Water, and Acetaldehyde

Volatile byproducts, or condensates, are generated from SSP reactions, and they are able to diffuse through the amorphous, crystal portion and then pellet surface. The removal of volatile byproducts is essential to build up longer molecular chains. Study on the distribution of these byproducts will bring about deeper understanding of SSP kinetic scheme. Figures 5, 6, and 7 delineate the spatial distribution of EG, water, and acetaldehyde inside pellets, respectively. The variance of the concentration of volatile byproducts can be seen clearly at different layers of a PET pellet. A few ppm of residual acetaldehyde (AA) is known to introduce an odor to PET beverage bottles, so generally AA content should be kept lower than 5 ppm. Previous mathematical models neglected the diffusion of AA for lacking of the experimental result of diffusion coefficient of AA. However, in our model, the diffusion coefficient is calculated and the diffusion of AA is involved in the model. Figure 8 shows the calculation results of AA distribution without considering the diffusion of AA, whereas Figure 7 is the results of AA distribution and the diffusion of AA is taken into account. The difference between Figures 7 and 8 is so obvious that it may be wrong to omit the diffusion of AA. The experimental measurements of the concentration of residual AA by Jabarin and Lofgren[3] was 5 ppm for Goodyear VFR-6014 solid stated 4 h at 230°C, which might be sufficient evidence.

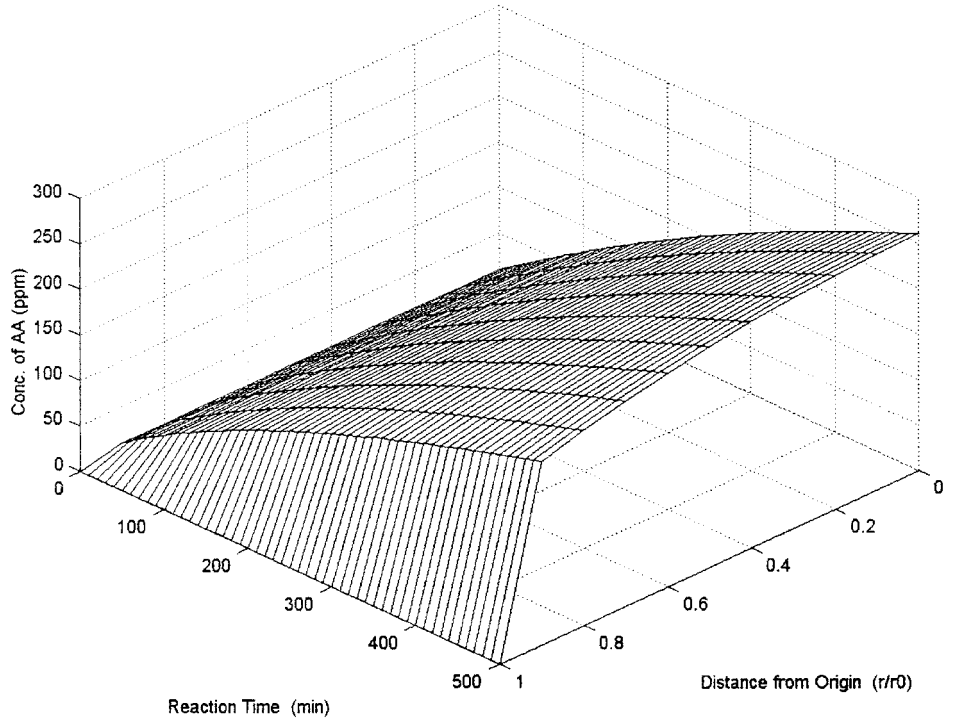

Figure 8. Distribution of concentration variance of acetaldehyde at different layers of a PET pellet under reaction temperature of 230°C without considering the diffusion of AA (C_{AA0} = 10 ppm, C_{AAs} = 0 ppm).

CONCLUSIONS

A comprehensive mathematical model was proposed for the PET SSP process to account of the effect of crystallinity, the influence of reactive chain mobility on reaction rates, and the diffusion of volatile byproducts ethylene glycol, water, and acetaldehyde. Compared with melting polymerization, PET SSP is a heterogeneous polymerization. As reactive end groups exist only in amorphous phase, increasing crystallinity can make the reaction rates more rapid, but at the same time reduces the diffusion rates of byproducts. The diffusion of volatile byproducts causes a mass loss of the reaction system. The model is validated by fitting against the experimental data reported in literature. The calculation results of the mathematical model give important clues for further experimental study on the optimization of PET SSP, the formation of byproducts such as DEG and acetaldehyde brings new strategies for SSP mechanism. The mathematical model can be used in analyzing other SSP processes for polymers such as polycaprolactam, polybutylene terephthalate, and others. However, further refinements of the present model need to be sought in the direction of the decrease of SSP reaction time to produce higher molecular weight polymers with improved physical and mechanical properties.

The authors greatly appreciate the financial support by Fok Ying Tung Education Foundation.

NOMENCLATURE

t	reaction time (min)
T	reaction temperature (K)
k_i	forward rate constant of reaction i (L/mol min)
K_i	equilibrium constant of reaction i
C_j	concentration of component j (mol/L)
$G_j(t)$	generation rate of component j due to chemical reactions at reaction time t
x_c	mass fraction crystallinity
M	mass of reaction system (mol/kg)
D_j	diffusion coefficient of amorphous fraction (cm^2/min)
D_{oj}	overall diffusion coefficient (cm^2/min)

λ	pellet shape factor
r	distance from origin of pellet (cm)
$r0$	distance from origin to surface of pellet (cm)
k_c	crystallization rate constant
x_{max}	maximum crystallinity
R_i (i = 1–9)	reaction rate of reaction i
$C_{amorphous}$	concentration of each component in amorphous fraction (mol/L)
$C_{overall}$	concentration of each component in amorphous and crystal fraction (mol/L)
m_p	chain mobility
E_p	activation energy of translational motion of polymer chains (kcal/mol)
C_1, C_2	constants in eq. (6)
T_g	glass translational temperature (K)
A_i	prefactor in eqs. (7) and (8)
E_i	activation energy of reaction i (kcal/mol)
A, B	constants in eq. (11)

REFERENCES

1. Chang, S.-Y.; Sheu, M.-F.; Chen, S.-M. J Appl Polym Sci 1983, 28, 3289–3300.
2. Chen, S.-A.; Chen, F.-L. J Polym Sci, Part A: Polym Chem 1987, 25, 533–549.
3. Jabarin, S. A.; Lofgren, E. A. J Appl Polym Sci 1986, 32, 5315–5335.
4. Ravindranath, K.; Mashelkar, R. A. Chem Eng Sci 1986, 41, 2197, 2969.
5. Chang, T. M. Polym Eng Sci 1970, 10, 364–368.
6. Devotta, I.; Mashelkar, R. A. Chem Eng Sci 1993, 48, 1859–1867.
7. Yoon, K. H.; Kwon, M. H.; Jeon, M. H.; Park, O. O. Polym J 1993, 25, 219–226.
8. Kang, C.-K.; Lee, B. C.; Ihm, D. W. J Appl Polym Sci 1996, 60, 2007–2015.
9. Ravindranath, K.; Mashelkar, R. A. J Appl Polym Sci 1990, 39, 1325–1345.
10. Tang, Z.-L.; Gao, Q.; Nan-xun, H.; Sironi, C. J Appl Polym Sci 1995, 57, 473–485.
11. Kang, C.-K. J Appl Polym Sci 1998, 68, 837–846.
12. Mallon, F. K.; Ray, W. H. J Appl Polym Sci 1998, 69, 1233–1250.
13. Schultz, J. M.; Fakirov, S. Solid State Behavior of Linear Polyester and Polyamides; Prentice Hall: Englewood Cliffs, NJ, 1990; pp 19–20.
14. Ravindranath, K.; Mashelkar, R. A. J Appl Polym Sci 1982, 27, 2625–2652.
15. Li, L.; Liu, Z.-H.; Huang, N.-X.; Yung, W.-X. Polym Adv Technol 2000, 11, 1–8.
16. Simonova, M. I.; Aizenshtein, E. M.; Shevchenko, V. V. Volokna 1973, 5, 14.
17. Gupta, S. A.; Kumar, A. Reaction Engineering of Step Growth Polymerization; Plenum Press: New York, 1987; p 252.
18. Schaaf, E.; Zimmermann, H.; Dietzel, W.; Lohmann, P. Acta Polym 1981, 32, 250.